The current issue and full text archive of this journal is available at
www.emeraldinsight.com/0961-5539.htm

Analysis of natural convection in a square cavity with a thin partition for linearly heated side walls

Received 28 February 2012
Revised 31 March 2013
Accepted 4 April 2013

M. Sathiyamoorthy
Department of Mathematics, Government Thirumagal Mills College, Gudiyatham, India, and
Ali J. Chamkha
Manufacturing Engineering Department, The Public Authority for Applied Education and Training, Shuweikh, Kuwait

Abstract

Purpose – The purpose of this paper is to optimize the heat transfer rate in square cavity by attaching fin at the bottom wall.
Design/methodology/approach – The problem is formulated and solved using finite element method. Accuracy of the method is validated by comparisons with previously published work.
Findings – It was found that attaching fin reduces heat transfer rate in the cavity.
Originality/value – Although the problem is not very original it is important in that many applications have heating on adjacent walls.

Keywords Square cavity, Rayleigh-Benard convection, Thin partition
Paper type Research paper

Nomenclature

l_p	length of the partition, m	T_c	temperature of cold at top edges of side walls, K
s_p	position of the partition at the bottom wall, m	T_h	temperature of hot (bottom) wall, K
L	length of the square cavity, m	*Greek symbols*	
L_p	dimensionless length of the partition, $=l_p/L$	θ	dimensionless temperature
S_p	dimensionless position of partition at the bottom wall, $=s_p/L$	ψ	stream function
n	the normal direction on a cavity wall	*Subscripts*	
Nu	local Nusselt number	b	bottom wall
$\overline{Nu}$	average Nusselt number	l	left wall
Pr	Prandtl number	r	right wall
Ra	Rayleigh number	s	side wall
T	fluid temperature, K	p	partition

1. Introduction

The phenomenon of natural convection flow in a cavity which is heated from below and cooled along the side walls have been studied numerically by several authors for

Authors would like to thank anonymous reviewers for constructive comments which improve the quality of the manuscript.

International Journal of Numerical Methods for Heat & Fluid Flow
Vol. 24 No. 5, 2014
pp. 1057-1072

0961-5539
DOI 10.1108/HFF-02-2012-0050

last three decades. This phenomenon often affects the thermal performance of many engineering and science applications such as boilers, nuclear reactor systems, energy storage, and conservation, fire control, and chemical, food and metallurgical industries. In this system the lighter fluid rises at middle of the hot bottom wall and gets heavier at the top wall and hence falls down along the cold side walls. Thus the fluid flow in this system is characterized by two recirculating cells which are symmetrical about the vertical line at the center of the bottom wall (Rayleigh-Benard convection). A comprehensive literature survey concerned with this subject is given in the papers (Ostrach, 1988; November and Nansteel, 1987; Valencia and Frederick, 1989; Ganzarolli and Milanez, 1995; Corcione, 2003). It is also noted that the RB instability strongly depends on the Prandtl number (*Pr*) of the fluids (Busse and Whitehead 1971, 1974; Busse and Clever, 1979). Recently, Sathiyamoorthy *et al.* (2007) have studied natural convection flow in a square cavity with uniformly heated bottom wall and linearly heated side walls while the top wall was kept insulated. In this is system also the fluid flow is characterized by RB convection cells for the Rayleigh numbers $Ra = 10^3$ and 10^4. For $Ra = 10^5$, a pair of secondary circulations are formed at the bottom of the cavity along with the RB convection cells and the intensities of secondary cells are depends totally on *Pr*.

The heat transfer rates in a heated cavity can be reduced either by adding porous medium in the cavity or by applying magnetic field or by attaching partitions and fins to the wall(s). The study of natural convection in a cavity by attaching partitions to the wall(s) received considerate attention in recent years. Tong and Gerner (1986) made a numerical study on natural convection in rectangular cavities with a vertical partition filled with air and found that partitioning is an effective method for reducing heat transfer. Maximum reduction in heat transfer occurs when the partition is placed midway between the vertical walls. Turkoglu and Yucel (1996) made a numerical study to investigate the conjugate natural convection in enclosures with vertical partitions. They searched the effects of number of partitions on natural convection and found that the mean Nusselt number decreases with increase in partition number. Nishimura *et al.* (1988) investigated the natural convection in enclosures with multiple vertical partitions both numerically and experimentally. Their results showed that the Nusselt number is inversely proportional to $(1 + N)$ where N is the number of partitions. They made a similar study in enclosures with an off-center partitions (Nishimura *et al.*, 1987); Ho and Yih (1987) made a numerical study on conjugate natural convection in an air-filled rectangular cavity with a partition. The study indicated that the heat transfer rate is considerably attenuated in a partitioned cavity in comparing with that for non-partitioned cavity. Acharya and Tsang (1985) made a study on natural convection in inclined enclosures with a centrally located partition. Recently (Kahveci, 2007a, b, c) investigated the natural convection in partitioned air filled enclosure using differential quadrature method. It was found that average Nusselt number increases with decreasing of thermal resistance of the partition and partition thickness has little effect on heat transfer. However, it may be noted that there exists no study on the RB instability in a square cavity with attached a partition on the bottom wall.

The present work analyses the effect of placing a thin partition on the Rayleigh-Benard instability in the square cavity for uniformaly heated bottom wall, linearly heated side walls and the top wall is well insulated. The thin partition is located in the bottom wall and it is either highly conductive or insulated with varying in length and position. The main objective is to determine the influence of partition's length and location on the modification of RB convection cells, secondary cells and isotherms which for $Ra = 10^5$

and also the dependents of the convection cells on Pr(0.7,100). Further, the partition's conductivity and insulation effects on the heat transfer rates are investigated in terms of average Nusselt numbers as a function of partition's length L_p for $Ra = 10^3$-10^5.

2. Problem formulation and governing equations

Consider a square cavity of length L with a vertical thin partition of length l_p placed at the bottom wall in the coordinate (s_p, 0) as shown in Figure 1. The bottom wall is uniformly heated with temperature T_h, the vertical walls are linearly heated with temperature profile $T_h-(T_h-T_c)y/L$ where $T_h > T_c$ and the top wall is well insulated. The thin partition can be either highly conductive material that maintains temperature at the temperature of the wall (T_h) or insulated. The thermophysical properties of the fluid in the flow model are assumed to be constant except for the density variations causing a body force term in the momentum equation. The Boussinesq approximation is assumed to be valid. The governing equations for the steady natural convection flow using conservation of mass, momentum and energy can be written in non-dimensional form as:

$$\frac{\partial U}{\partial X} + \frac{\partial V}{\partial Y} = 0 \tag{1}$$

$$U\frac{\partial U}{\partial X} + V\frac{\partial U}{\partial Y} = -\frac{\partial P}{\partial X} + Pr\left(\frac{\partial^2 U}{\partial X^2} + \frac{\partial^2 U}{\partial Y^2}\right) \tag{2}$$

$$U\frac{\partial V}{\partial X} + V\frac{\partial V}{\partial Y} = -\frac{\partial P}{\partial Y} + Pr\left(\frac{\partial^2 V}{\partial X^2} + \frac{\partial^2 V}{\partial Y^2}\right) + RaPr\theta \tag{3}$$

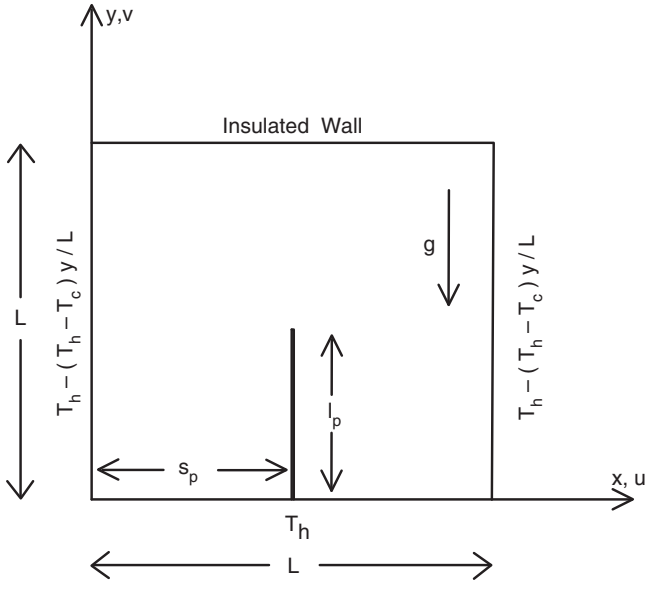

Figure 1.
A square cavity with a thin partition attached vertically at the bottom wall

$$U\frac{\partial\theta}{\partial X}+V\frac{\partial\theta}{\partial Y}=\left(\frac{\partial^2\theta}{\partial X^2}+\frac{\partial^2\theta}{\partial Y^2}\right) \tag{4}$$

with the following boundary conditions.

On the walls:

$$\begin{aligned} &U(X,0)=U(X,1)=U(0,Y)=U(1,Y)=0\\ &V(X,0)=V(X,1)=V(0,Y)=V(1,Y)=0\\ &\theta(X,0)=1,\ \frac{\partial\theta}{\partial Y}(X,1)=0\\ &\theta(0,Y)=1-Y,\ \theta(1,Y)=1-Y \end{aligned} \tag{5}$$

On the thin partition:

$$U=V=0,\theta=1(\text{conductive})\text{ or }\frac{\partial\theta}{\partial n}=0(\text{insulated}) \tag{6}$$

The non-dimensional variables are given by:

$$\begin{aligned} &X=\frac{x}{L},\ Y=\frac{y}{L},\ U=\frac{uL}{\alpha},\ V=\frac{vL}{\alpha},\ \theta=\frac{T-T_c}{T_H-T_c}\\ &P=\frac{pL^2}{\rho\alpha^2},\ Pr=\frac{\nu}{\alpha},\ Ra=\frac{g\beta(T_H-T_c)L^3Pr}{\nu^2} \end{aligned} \tag{7}$$

The dimensionless length of the partition is defined as $L_p=l_p/L$. The partition is attached at bottom wall with dimensionless coordinate defined as ($S_p=S_p/L$,0). From the above equations, the dimensionless parameters of the problem are Ra, Pr, L_p and S_p.

3. Computational method and the rate of heat transfer

In order to determine the flow and heat transfer in the cavity the penalty finite element method is used. To solve the non-dimensional governing Equations (1)-(4) along with the boundary conditions (5)-(6), the nine node bi-quadratic elements are used to get smooth solutions. A detailed description of the procedure is presented in references Sathiyamoorthy and Ali (2012). The numerical solutions are obtained in terms of velocity components (U, V) and temperature (θ). The fluid motion is displayed using the stream function (ψ) obtained from the velocity components U and V. The relationship between the stream function and velocity components are $U=\partial\psi/\partial Y$ and $V=-\partial\psi/\partial X$, which yields a single Poisson equation:

$$\frac{\partial^2\psi}{\partial X^2}+\frac{\partial^2\psi}{\partial Y^2}=\frac{\partial U}{\partial Y}-\frac{\partial V}{\partial X} \tag{8}$$

It may be noted that the positive sign of ψ denotes anticlockwise circulation and the clockwise circulation is represented by the negative sign of ψ. The Galerikin finite

element method is used to solve the linear Equation (8). The no-slip condition is valid at all boundaries as there is no cross-flow, hence $\psi = 0$ is used for the boundaries.

The heat transfer coefficient at solid walls of the cavity (local Nusselt number) is defined by:

$$Nu = -\frac{\partial \theta}{\partial n} \tag{9}$$

where n denotes the normal direction on a plane. The local Nusselt number at bottom wall (Nu_b) and at the side wall (Nu_s) are evaluated. The average Nusselt numbers at the bottom and side walls are computed as follows:

$$\overline{Nu_b} = \int_0^1 Nu_b dX \quad and \quad \overline{Nu_s} = \int_0^1 Nu_s dY \tag{10}$$

4. Code validation and parameters for numerical simulation

In the finite element based code, the square domain consists of 20×20 uniform bi-quadratic elements which correspond to 41×41 uniform grid points. The bi-quadratic elements with lesser number of nodes smoothly capture the non-linear variations of the filed variables. The full details of the method can be found in a brief discription is given in our previous work (Sathiyamoorthy and Ali, 2012). The code without partition was tested and verified via comparing the results with the benchmark solutions Vahl Davis (1983) for $Ra = 10^3 - 10^5$ and the results were in well agreement. Table I gives the values of the mean Nusselt number for the left or right walls for a square cavity and these values were in excellent agreement with those reported earlier (Vahl Davis, 1983; Nag *et al.*, 1993; Shi and Khodadahi, 2003). Another test was conducted with a thin partition attached on the hot left wall which has been investigated by Shi and Khodadahi (2003) for a differentially heated square cavity. The agreement was very satisfactory for the hot thin partition of length $L_p = 0.5$ located at middle of the hot wall. For instance when $Ra = 10^5$ and $Pr = 0.707$, the maximum of absolute value of the stream functions at the primary vortex was $|\psi|_{max} = 10.435$ obtained by current study, while that reported by Xundan Shi and Khodadadi was 10.456 for 80×80 uniform grid system. The computation have been carried out for various length of thin partition $L_p = 0.25$, 0.5 and 0.75 with positions $S_p = 0.25$ and 0.5 for $Ra = 10^5$ and $Pr = 0.7$-1000.

5. Results and discussions

5.1 Stream functions and isotherms

5.1.1 Without partition. The present natural convection flow problem in the non-partitioned cavity has been studied already by Sathiyamoorthy *et al.* (2007).

Ra	10^4	10^5	10^6
Vahl Davis (1983)	2.243	4.519	8.800
Nag *et al.* (1993)	2.240	4.510	8.820
Shi and khodadahi (2003)	2.247	4.532	8.893
Present study	2.253	4.584	8.921

Sources: Vahl Davis (1983), Nag *et al.* (1993), Shi and khodadahi (2003)

Table I. Comparison of the predicted Nusselt number $\overline{Nu}$ on the left or right walls of the cavity without thin partition with references

They found the Rayleigh-Benard instability in the cavity for $Ra = 10^3$ and 10^4. i.e a pair of symmetrical recirculating cells are formed within the cavity. With increasing Ra to 5×10^4 for $Pr = 0.7$, due to the additional heat from lower part of side walls to the cavity, another pair of secondary cells are formed at the corners of the bottom wall. Figures are not shown for these cases as they are appeared in the paper (Sathiyamoorthy *et al.*, 2007). Further, at $Ra = 10^5$ for $Pr = 0.7$, the secondary cells are established as two symmetrical RB convection cells in the lower part of the cavity and circulating in the opposite directions of the primary RB cells as seen in the Figure 2(a). Thus the primary cells are compressed and pushed in the upper part of the cavity and, "hot" and "cold" fluid regimes appears distinctly across the temperature contour $\theta = 0.6$. The maximum intensity of the lower and upper cells are $|\psi|_{max} = 3.44$ and 6.33, respectively. For the higher value of Prandtl number, $Pr = 100$, the flow momentum transport much faster than the thermal transfer, which implies the primary RB convection cells becomes stronger with $|\psi|_{max} = 11.10$ (Figure 2(b)). So the lower cells are cornered and the isotherms becomes crowded and close to the linearly heated walls with apparent symmetry. Which implies that the RB instability is strongly dependent on Pr of the fluids.

5.1.2 Partition in the middle. Figures 3 and 4 elucidates the features of locating insulated and conductive partitions in the middle of the bottom wall ($S_p = 0.5$) with

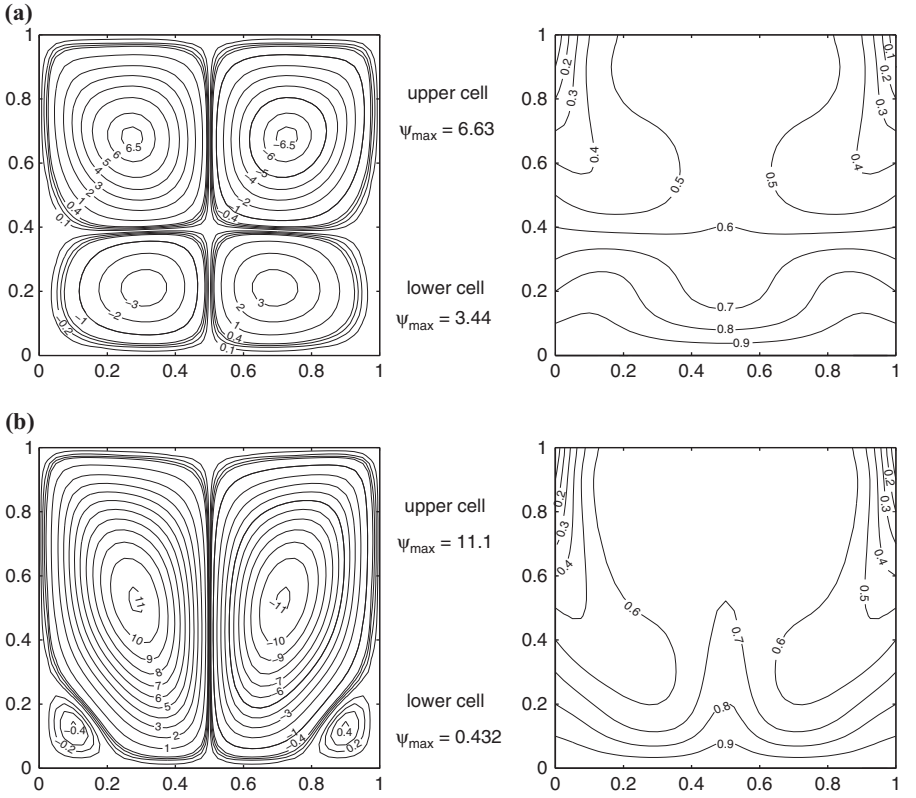

Figure 2.
Streamlines and isotherms of $Ra = 10^5$ without partition

Notes: (a) Pr=0.7 and (b) Pr=100

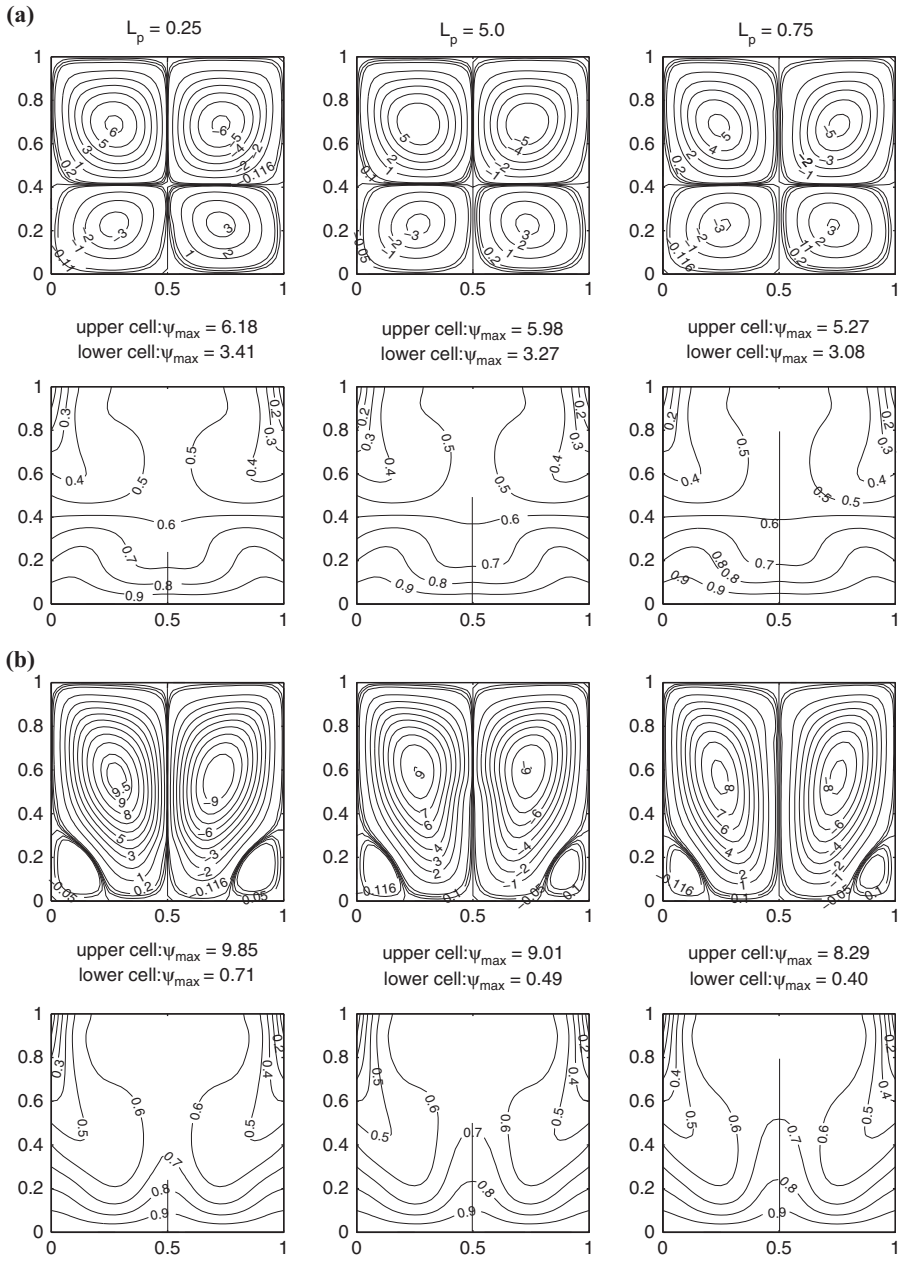

Notes: (a) $Pr = 0.7$ and (b) $Pr = 100$

Figure 3.
Streamlines and isotherms of $Ra = 10^5$ with insulated partition of various length located at $S_p = 0.5$

different length ($L_p = 0.25, 0.5, 0.75$) on streamline and isotherm contours for $Ra = 10^5$ and two different value of Pr(0.7 and 100). Locating the insulated partition in the middle of the bottom wall does not alter the Rayleigh-Benard convection cells, secondary cells and the isotherms those are formed in the non-partitioned cavity as

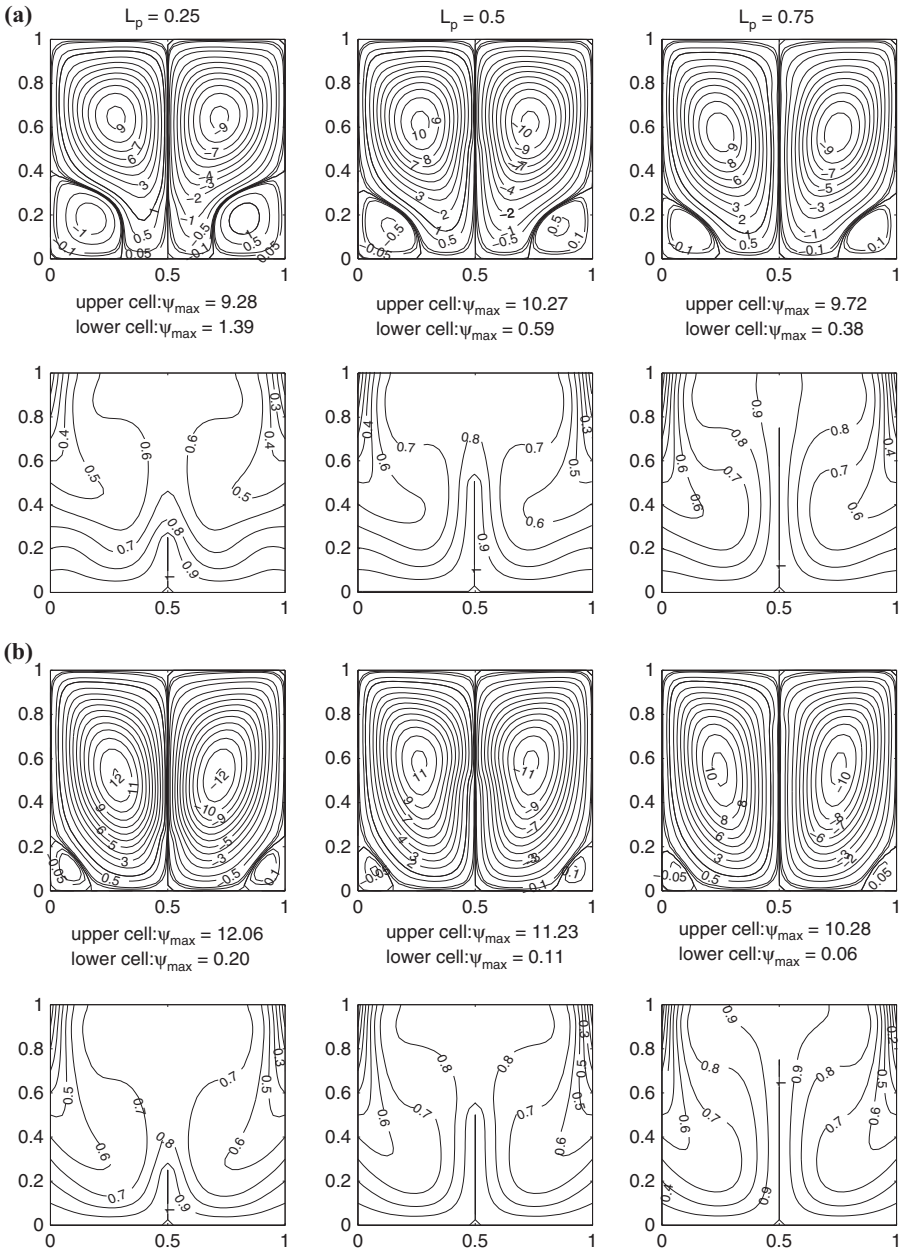

Figure 4.
Streamlines and isotherms of $Ra = 10^5$ with conductive partition of various length located at $S_p = 0.5$

Notes: (a) $Pr = 0.7$ and (b) 100

seen in Figure 3. However, the maximum intensity of cells ($|\psi|_{max}$) decreases slowly with increasing the length of the partition L_p. Thus, the only mechanism is the separation of the cavity for locating a insulated partition at the middle of the bottom wall. For conductive partition case, due the additional heat from the conductive

partition, the primary RB cells dominates the cavity (see Figure 4). Which implies that the maximum intensity of primary RB convection cell ($|\psi|_{max}$) increases with respective to the length and the secondary cells are cornered at the bottom wall of the cavity for both *Pr*. Moreover, the higher values of isotherms are shifted along the side walls as the partition length increases. So there is a another mechanism for conduction partition case which is the additional heat to the cavity. Here also the RB convection cells are dependent strongly on *Pr* irrespective of length (L_p) for both type partitions.

5.1.3 Partition on the side. Figures 5 and 6 shows similar results as those presented in Figures 3 and 4 but the partitions are located on the side of the bottom wall ($S_p = 0.25$). As seen Figure 5, the presence of the conductive partition at $S_p = 0.25$ results the absence of the Rayleigh-Benard instability and a small circulation instead is formed at the bottom right corner of the cavity. Again, as the length of the partition L_p increases, the bigger cell to the right side of the partition becomes stronger while the smaller cell to the left side of the partition becomes weaker and stretched more along the side wall. Also, the small circulation instead becomes smaller and weaker as L_p increases. This is true for both $Pr = 0.7$ and 100. However, it is observed that for $Pr = 100$, $L_p = 0.25$, the cell to the left side of the partition is rotating at a faster rate and the cell to the right side of the partition is rotating at a slower rate than the one corresponding to $Pr = 0.7$. But for $L_p = 0.5$ and 0.75, the corresponding convection cells becomes identical. i.e, the dependence of convection cells on *Pr* becomes weaker as the length increases due to the absence of RB instability. In addition, the higher value of isotherm ($\theta \geqslant 0.7$) that occurred along the bottom wall in the non-partitioned cavity are shifted along the side walls as L_p increases for both *Pr*. Which implies that as length of the partition increases, the gradient of temperature increases at side wall and decreases at the bottom wall. Thus, placing the conductive partition at the side of the bottom wall causes two important mechanisms, one is the alteration of the the four cells, while the other is additional heat from the partition to the cavity.

When the partition is insulated and $Pr = 0.7$, a different cellular behavior is predicted for $L_p = 0.25$ (Figure 6). Two main cells with two secondary eddies are predicted in which the strongest clockwise rotating cell is extended diagonally from the top left corner to the bottom right corner of the cavity. As L_p increases to 0.5 and 0.75, the flow patterns are similar to the case of conductive partitions with corresponding lengths $L_p = 0.5$ and 0.75. However, the intensity of the counter-clockwise rotating cell increases considerably and the clockwise rotating cell becomes more confined compared to the case of conductive partition. For this case, the isotherms shows significant distortions as L_p increases. When *Pr* increases to 100 for $L_p = 0.25$, a significantly different streamlines behavior is predicted in which the two main counter-rotating cells are almost of equal intensities. However, as L_p increases, similar features as for the case $Pr = 0.7$ are observed but with lower intensity of the counter-clockwise rotating cell and increased intensity of the circulation instead at the bottom right corner of the cavity. i.e, the convection cells that occurred on the right side of partition depends on *Pr*. Moreover, on contrast to the case of conductive partition, the shifting of the isotherms along the side walls is very less as the length of insulated partition increases. Thus, placing the insulated partition on the side of the bottom wall alters the RB instability only.

5.2 Heat transfer rates

5.2.1 Partition in the middle. Figure 7(a, b, c) illustrate the overall effects on the heat transfer for the conductive and insulated partitions which are located in the middle of

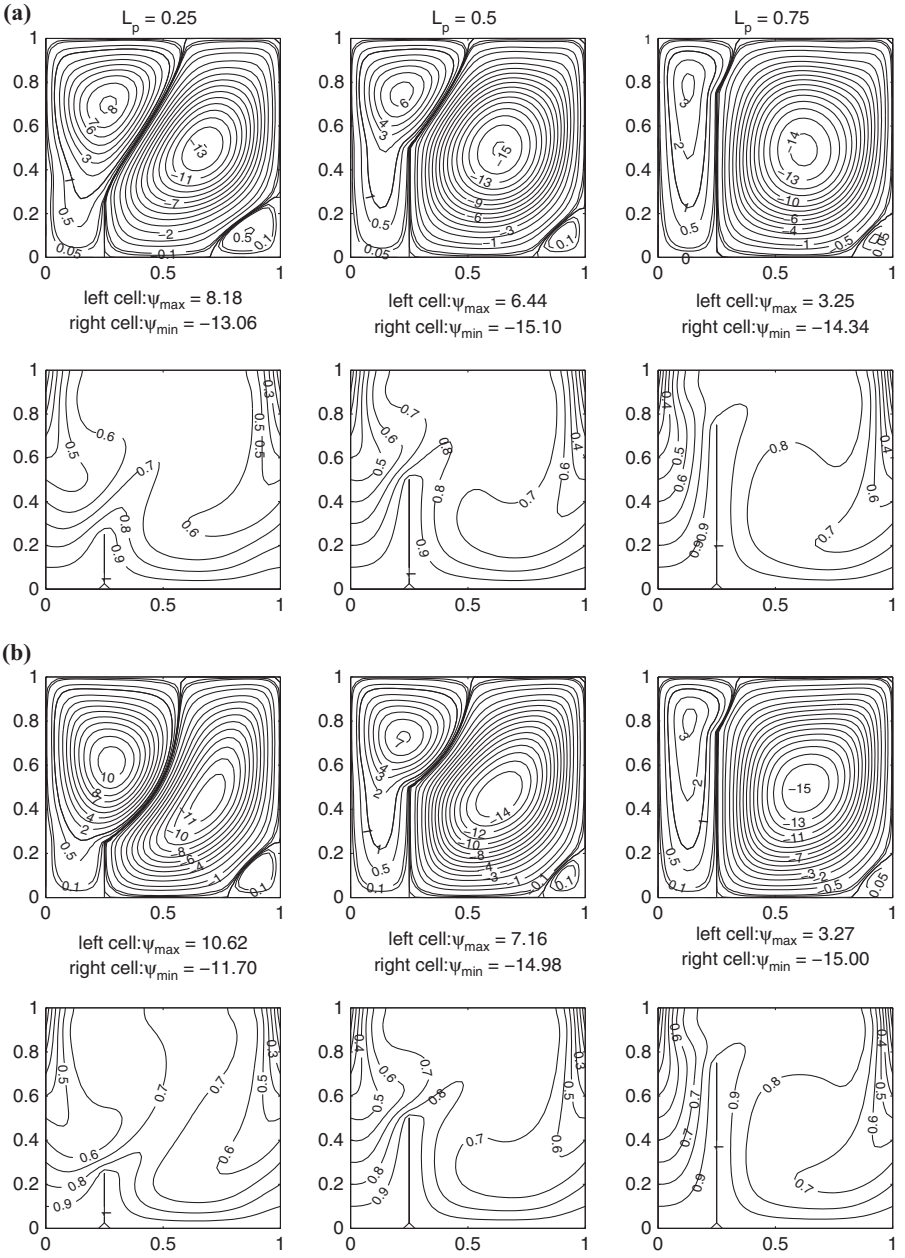

Figure 5.
Streamlines and isotherms of $Ra = 10^5$ with conductive partition of various length located at $S_p = 0.25$

Notes: (a) $Pr = 0.7$ and (b) 100

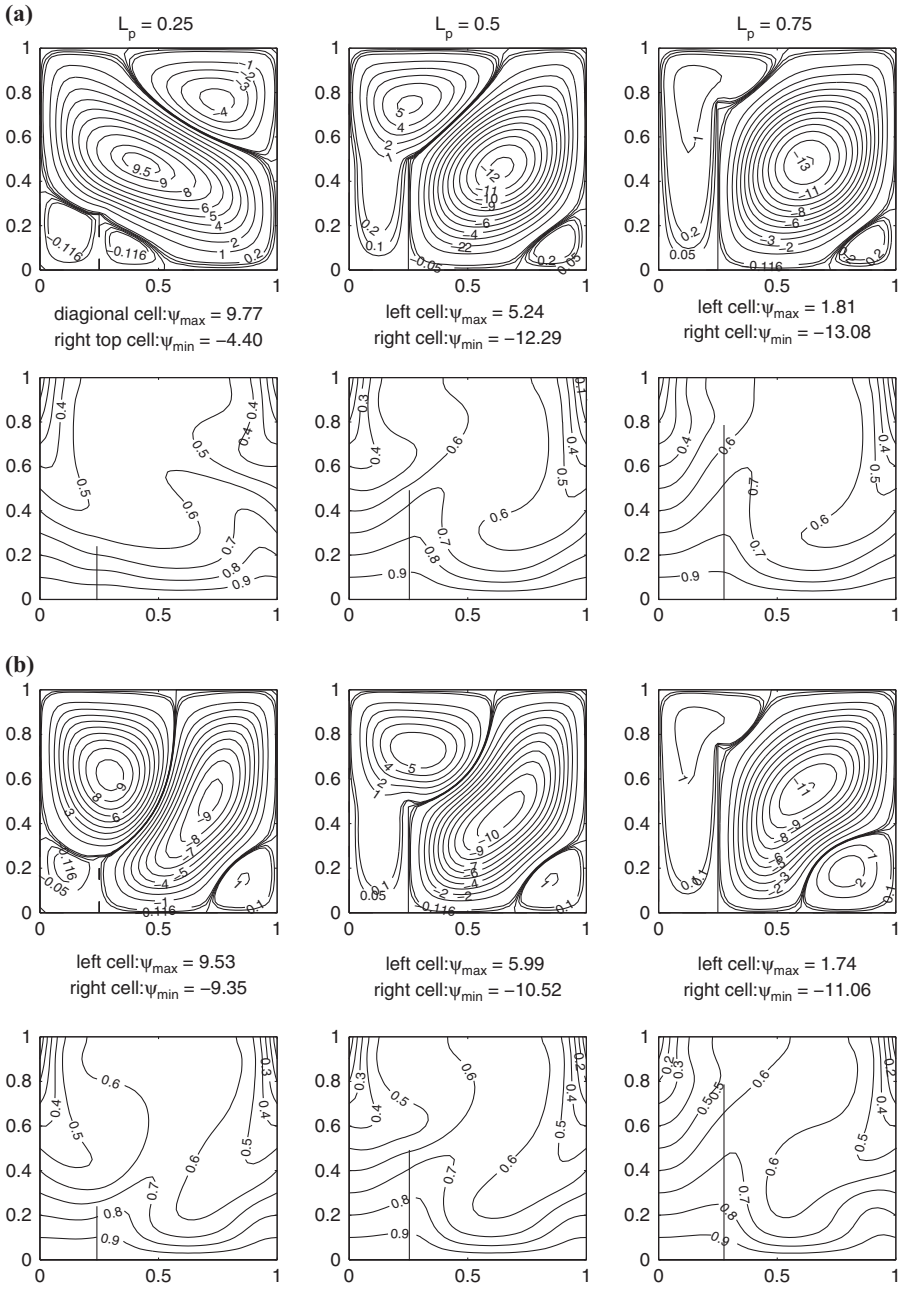

Notes: (a) $Pr = 0.7$ and (b) 100

Figure 6.
Streamlines and isotherms of $Ra = 10^5$ with insulated partition of various length located at $S_p = 0.25$

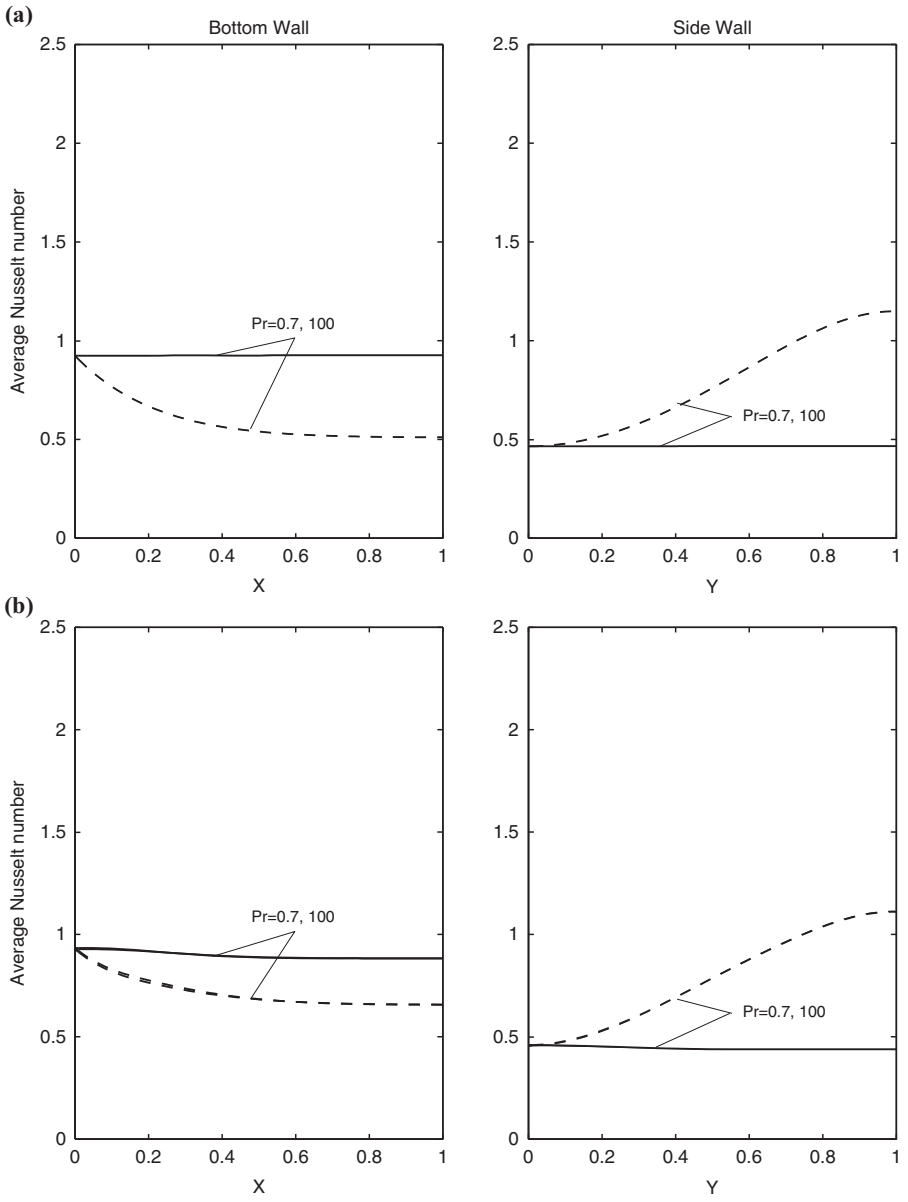

Notes: (a)10^3, (b)10^4 and (c)10^5 (insulated (—) and conductive (----))

Figure 7.
Variation of average Nusselt number along the bottom and side walls as a function of partition's length (insulated and conductive), located in the middle of the bottom wall

bottom wall ($S_p = 0.5$), where the average Nusselt numbers are plotted verses partitions length (L_p) for the parameters of Rayleigh numbers $Ra = 10^3$, 10^4 and 10^5 with $Pr = 0.7$ and 100. As the partitions located on the middle of uniformly heated bottom wall and the boundary conditions at side walls identical, the average Nusselt numbers at the side walls are equal. For $Ra = 10^3$ and 10^4 (conduction-dominated

regime and moderate convection regime), the average Nusselt number at the bottom wall decreases and that increases along the side wall significantly as conductive partition length L_p increases. However, when the partition is insulated, the average Nusselt numbers for both walls does not change as L_p increases. This is due to shifting of isotherms along the side walls which increases at a higher rate for conductive partition while that increases at low rate for insulated partition. Moreover, the average Nusselt numbers of Pr(0.7,100) are identical for both case of partitions as the convection regimes are moderate.

For $Ra = 10^5$ (convection dominated regime), the influence of Pr on the average Nusselt number is predicted for both case of partitions. i.e, as Pr increases from 0.7 to 100, the average Nusselt number on the bottom and side walls increases for all length (L_p) (see Figure 7(c)). For $Ra = 10^5$, the average Nusselt number changes as the insulated partition length L_p increases which is contrary to $Ra = 10^3$ and 10^4. Also, it is interesting to note that the average Nusselt number attains minimum at $L_p = 0.1$ on both the walls for conductive partition and $Pr = 0.7$. Looking to overall Figure 7, it is predicted that the average Nusselt number increases as Ra increases. Moreover, locating the insulation partition at the middle of the bottom wall reduces the average Nusselt number on both walls is at a less rate as the length of the partition increases.

5.2.2 Partition on the side

Figure 8(a, b, c) shows the influence of the partition's length L_p on the average Nusselt number for the same parameters of the Figure 7(a, b, c). But the partitions are located on the sides of the bottom wall ($S_p = 0.25$). Thus the average Nusselt numbers are different for both side walls. It is also observed that different trends of the average Nusselt numbers are predicted for different parametric conditions. For conductive partition and $Ra = 10^3$ and 10^4, the average Nusselt number decreases at the bottom wall and that increases along the side walls significantly as the length of partition increases (Figure 8(a, b)). But, as the partition is located on the left side of the bottom wall, the rate of increase is more for the left wall than that of right wall. On the contrary, for insulated partition and $Ra = 10^4$, the average Nusselt number increases and decreases at the same rate along the left and right walls, respectively.

Finally, in Figure 8(c) for $Ra = 10^5$ with $Pr = 0.7$ and 100, when the partition is conductive the behavior of the average Nusselt numbers for the bottom, left and right walls are more like the ones for the case of $Ra = 10^4$. For insulated partition and $Pr = 0.7$, the average Nusselt number oscillates as L_p increases for all walls. This is due to the continuous changes of flow directions in the cavity as L_p increases (see Figure 6(a)). Except for this case, the overall heat transfer rate at the bottom wall decreases at a same rate for both locations with respective to the partition type (compare Figures 7 and 8).

6. Conclusions

(1) Placing any partition in the middle of the bottom wall of the cavity does not alter the Rayleigh-Benard convection cells. The maximum intensity of the RB convection cells strongly depend on the length for conductive partition and the dependent cell becomes weak for insulated partition. Also, the RB convection cells strongly depend on the Pr of the fluids.

(2) In general, locating any partition on the side of the bottom wall results one stronger cell to the right side of the partition and another weaker cell to the left side of the partition and the absence of the Rayleigh-Benard instability.

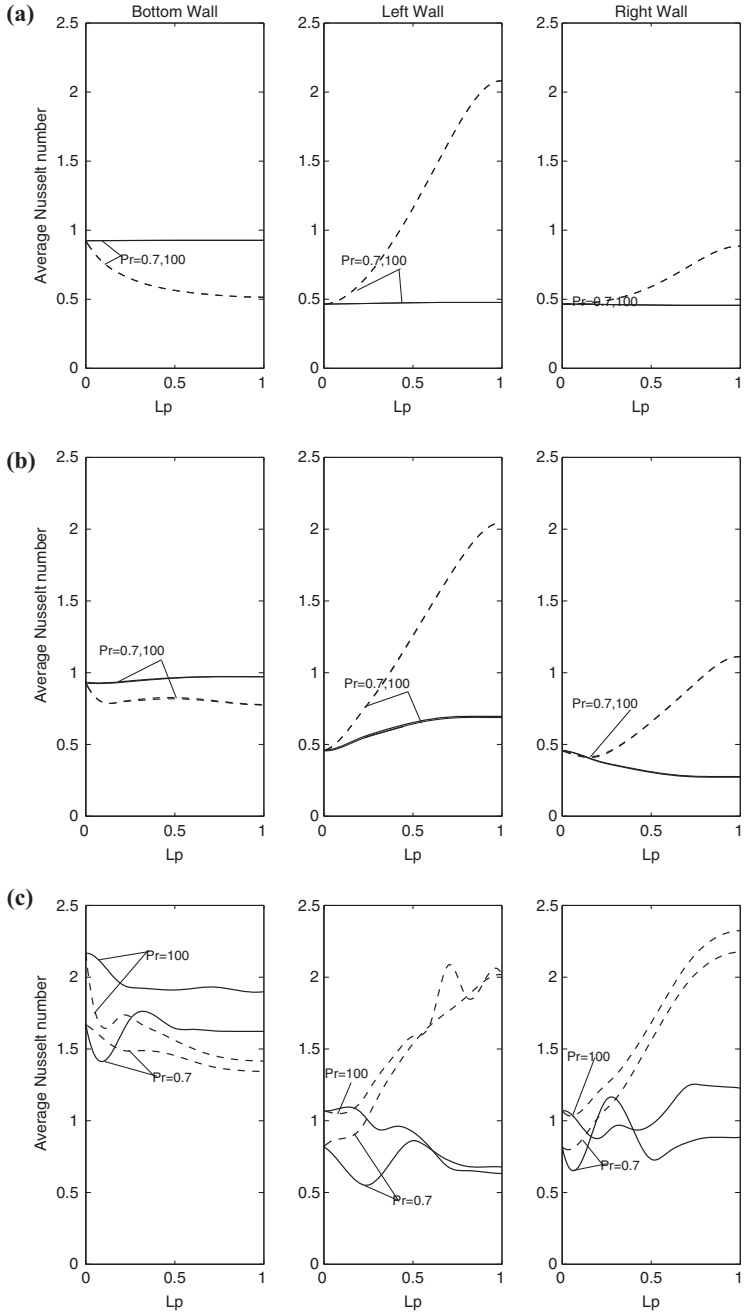

Notes: (a)10^3, (b)10^4 and (c)10^5 (insulated (—) and conductive (----))

Figure 8.
Variation of average Nusselt number along the bottom, left and right walls as a function of partition's length (insulated and conductive), located on the side of the bottom wall

For both partitions, the maximum intensities of the convection cells dependent strongly on the length. The dependance of convection cells on *Pr* becomes weaker as the length of conductive partition increases.

(3) The convection cell gains heat from conductive partition and the higher value of isotherms gets shifted along the side walls. This produces low-heat transfer at the bottom wall and high-heat transfer along the side walls with respective to the length.

(4) The average Nusselt numbers of *Pr*(0.7,100) are identical for both case of partitions and $Ra = 10^3$-10^4. But, the influence of *Pr* on average Nusselt number are also identified for $Ra = 10^5$.

(5) Finally, for attaching conductive partition in any location, the rate of heat transfer rate decreases and increases at the bottom and side walls, respectively. It is also concluded that locating the insulation partition in the midway of the bottom wall reduces the heat transfer rates on both walls at a less rate for $Ra = 10^5$.

References

Acharya, S. and Tsang, C.H. (1985), "Natural convection heat transfer in a fully partitioned inclined enclosure", *Numerical Heat Transfer: Part-A*, Vol. 9 No. 4, pp. 407-428.

Busse, F.H. and Clever, R.M. (1979), "Instabilites of convection rolls in a moderate prandtl number fluids", *Journal of Fluid Mechanics*, Vol. 91 No. 2, pp. 319-335.

Busse, F.H. and Whitehead, J.A. (1971), "Instabilites of convection rolls in a high Prandtl number fluids", *Journal of Fluid Mechanics*, Vol. 47 No. 2, pp. 305-320.

Busse, F.H. and Whitehead, J.A. (1974), "Oscillatery and collactive instabilites for large Prandtl number convection", *Journal of Fluid Mechanics*, Vol. 66 No. 1, pp. 67-79.

Corcione, M. (2003), "Effects of the thermal boundary conditions at the sidewalls upon natural convection in rectangular enclosures heated from below and cooled from above", *International Journal of Thermal Sciences*, Vol. 42 No. 2, pp. 199-208.

Ganzarolli, M.M. and Milanez, L.F. (1995), "Natural convection in a rectangular enclosures heated from below and symmetrically cooled from the sides", *International Journal of Heat and Mass Transfer*, Vol. 38 No. 6, pp. 1063-1073.

Ho, C.J. and Yih, Y.L. (1987), "Conjugate natural heat transfer in an air-filled rectangular cavity", *International Communication in Heat and Mass Transfer*, Vol. 14 No. 1, pp. 91-100.

Kahveci, K. (2007a), "Natural convection in a partitioned vertical enclosure heated with a uniform heat flux", *ASME Transaction Journal of Heat Transfer*, Vol. 129 No. 6, pp. 717-726.

Kahveci, K. (2007b), "A differential quadrature solution of natural convection in an enclosure with a finite-thickness partition", *Numerical Heat Transfer: Part-A*, Vol. 52 No. 10, pp. 1009-1026.

Kahveci, K. (2007c), "Numerical simulation of natural convection in a partitioned enclosure using PDQ method", *International Journal of Numerical Methods for Heat and Fluid Flow*, Vol. 17 No. 4, pp. 439-456.

Nag, A., Sarkar, A. and Sastri, V.M.K. (1993), "Natural convection in a differentially heated square cavity with horziontal plate on the hot wall", *Computational Methods and Applied Mechanical Engineering*, Vol. 110 No. 4, pp. 143-156.

Nishimura, T., Shiraishi, M. and Kawamura, Y. (1987), "Natural convection heat transfer in enclosures with an off-center partition", *International Journal of Heat and Mass Transfer*, Vol. 30 No. 8, pp. 1756-1758.

Nishimura, T., Shiraishi, M., Nagasawa, F. and Kawamura, Y. (1988), "Natural convection heat transfer in enclosures with multiple vertical partitions", *International Journal of Heat and Mass Transfer*, Vol. 31 No. 8, pp. 1679-1686.

November, M. and Nansteel, M.W. (1987), "Natural convection in rectangular enclosures heated from below and cooled along one side", *International Journal of Heat and Mass Transfer*, Vol. 30 No. 11, pp. 2433-2440.

Ostrach, S. (1988), "Natural convection in enclosures", *ASME Transaction Journal of Heat Transfer*, Vol. 110 No. 4b, pp. 1175-1190.

Sathiyamoorthy, M. and Ali, C. (2012), "Natural convection flow under magnetic field in a square cavity for uniformly (or) linearly heated adjacent walls", *International Journal of Numerical Methods for Heat and Fluid Flow*, Vol. 22 No. 5, pp. 677-698.

Sathiyamoorthy, M., Basak, T., Roy, S. and Pop, I. (2007), "Steady natural convection flows in a square cavity with linearly heated side wall(s)", *International Journal of Heat and Mass Transfer*, Vol. 50 Nos 3-4, pp. 766-775.

Shi, X. and Khodadahi, J.M. (2003), "Laminar natural convection heat transfer in differentially heated square cavity due to thin partition on the hot wall", *ASME Transaction Journal of Heat Transfer*, Vol. 125 No. 4, pp. 624-634.

Tong, T.W. and Gerner, F.M. (1986), "Natural convection in partitioned air-filled rectangular enclosures", *International Communication in Heat and Mass Transfer*, Vol. 13 No. 1, pp. 99-108.

Turkoglu, H. and Yucel, N. (1996), "Natural convection heat transfer in enclosures with conducting multiple partitions and side walls", *Journal of Heat Mass Transfer*, Vol. 32 Nos 1-2, pp. 1-8.

Vahl Davis, G.D. (1983), "Natural convection of air in a square cavity: a bench mark numerical solution", *International Journal of Numerical Methods in Fluids*, Vol. 3 No. 3, pp. 249-264.

Valencia, A. and Frederick, R.L. (1989), "Heat transfer in a square cavities with partially active vertically walls", *International Journal of Heat and Mass Transfer*, Vol. 32 No. 8, pp. 1567-1574.

Corresponding author
Dr M. Sathiyamoorthy can be contacted at: m.sathiya@yahoo.com